Age and Magnitude of Dip-Slip Faulting Deduced from Differential Cooling Histories: An Example from the Hope Fault, Northwest Montana[1]

Jeffrey A. Fillipone[2], An Yin, T. Mark Harrison, George Gehrels[3],
Moe Smith[3], and James C. Sample[4]

Department of Earth and Space Sciences, University of California,
Los Angeles, California 90024-1567

ABSTRACT

Determination of the age of fault motion poses a challenge in tectonics, yet rarely produces satisfactory results. We describe a new method in which the age and magnitude of dip-slip faulting are estimated from contrasting cooling histories of footwall and hanging wall rocks adjacent to the Hope fault, northwest Montana. The Hope fault has been interpreted in the past as a mostly right-slip fault. New kinematic data, $^{40}Ar/^{39}Ar$ thermochronometry, and geobarometry indicate that cooling of footwall rocks at ~40 Ma resulted from dip-slip movement. This movement caused vertical separation of about 3 to 5 km between footwall and hanging wall rocks, suggesting that a minimum dip-slip component of 4 km developed during the Late Eocene. These results indicate that the Hope fault experienced substantial normal slip in the Late Eocene, making it coeval with other normal and detachment-style faults in the northern U.S. Cordillera. The western Lewis and Clark line, which in part may share a common tectonic history with the Hope fault, should be re-evaluated for its role in transferring Tertiary extension between the Priest River and Bitterroot core complexes.

Introduction

When unraveling the geologic history of a region, geologists frequently must determine the age and magnitude of fault motion. Traditional approaches have relied on determining: (1) the ages of pre-, syn-, and post-faulting plutons (e.g., Coney 1980); (2) the age of syn-faulting sediments (e.g., Wiltschko and Dorr 1983), and (3) the age of fault gouge (Lyons and Snellenburg 1971). The first scheme can constrain fault age if intrusion occurs close to the time of faulting; an ideal but rare circumstance. The second scenario is limited by the fact that syn-faulting sediments commonly are lost to erosion. Besides problems of protolith contamination and thermal stability of gouge products, the third method may only date the last episode of

faulting; thus a general method is needed that can provide the age and magnitude of fault motion. In the present approach, faulting has juxtaposed pre-kinematic plutons with different conductive cooling histories, which we exploit in estimating the vertical component of fault displacement (i.e., throw). Through application of $^{40}Ar/^{39}Ar$ thermochronometry, the cooling histories of these rocks are recovered and used to help reconstruct the dip-slip fault history. Such an approach provides a generally applicable method of determining the age and magnitude of dip-slip faulting. We illustrate the method with an example from the Hope fault in northwest Montana. The movement history of the Hope fault is controversial; different kinematic interpretations (Harrison et al. 1986; Yin 1991) and their implications for regional tectonics (Rehrig et al. 1987; Harms and Price 1992) make the Hope fault an interesting object for application of our method. Differential cooling histories of footwall and hanging wall rocks determined by $^{40}Ar/^{39}Ar$ thermochronometry were found to be compatible with field observations that suggest as much as 10

km of accumulated dip-slip in the Late Eocene. We conclude that movement on the Hope fault was coeval with the development of other normal fault systems in the region, suggesting that linkage among Eocene extensional fault systems is plausible, and these findings call into question the importance of strike-slip along the Hope fault and the western Lewis and Clark line.

Regional Tectonic Setting

Variously interpreted to be strike-slip or normal-slip, Precambrian to Cenozoic, the Hope fault and its role in the evolution of the northern U.S. Cordillera have been controversial. The southwest-dipping Hope fault lies at the northern end of the western Lewis-Clark line/fault system (Billingsley and Locke 1939; Harrison et al. 1972; Harrison et al. 1986) but originally was thought not to be part of the Lewis and Clark line (Billingsley and Locke 1939). Many workers, however, believe its evolution was closely linked to that of the Lewis and Clark line (e.g., Smith 1965; Reynolds 1979; Harrison et al. 1986). Based on the Hope fault's physiographic similarity to the southern Rocky Mountain trench normal faults, Pardee (1950) proposed that it was a late Cenozoic normal fault. About 26 km of right-lateral horizontal separation in northern Idaho and northwestern Montana was suggested by Harrison and Jobin (1963). They interpreted the separation as slip that began during deposition of middle Proterozoic Belt Supergroup strata. Harrison et al. (1972) suggested that 4–7 km of the 26 km right slip may have occurred in the early Tertiary. More recently, it was suggested that the Hope fault acted as a right-slip transfer fault during late Cretaceous to early Tertiary thrusting (Harrison et al. 1986), and later during Eocene core complex extension (Rehrig et al. 1987; Doughty and Sheriff 1992; Hodges and Applegate 1993). Results from recent mapping (Yin 1991) and laboratory studies (Fillipone et al. 1992) suggest that the Hope fault experienced dominantly normal slip from Late Eocene to perhaps the Early Oligocene.

Kinematics of the Hope Fault

The Hope fault zone is best exposed along the Clark Fork River near Blueslide, Montana (Harrison et al. 1986: loc. 1, figure 1), where it juxtaposes lower Striped Peak Formation (upper Belt) over Prichard Formation (lower Belt). The Prichard Formation is strongly brecciated and fractured along the well-exposed fault surface. The Hope fault zone at this locality dips 28°–35° southwest,

which is much shallower than estimated in previous reports (Harrison et al. 1972, 1986). Minor fault surfaces immediately below the main fault are grooved and striated, with local fibrous quartz veining and slickensides. The dominant attitude of these striations is down-dip (figure 1). In the foot-wall of the Hope fault 2 km northwest of Hope, Idaho (location 2, figure 1), numerous southwest-dipping minor normal faults cut the Prichard Formation and offset the Hope sills (figure 1). At Webb Creek, Idaho (loc. 3, figure 1) the Hope fault juxtaposes younger Wallace Formation over older Prichard Formation. The average orientation of striations measured on shear surfaces in the fault zone is 220°/66°; that fact, when coupled with the sense of stratigraphic offset, indicates dip slip. Using thicknesses of upper, middle, and lower Belt Supergroup strata from Harrison et al. (1986) in conjunction with the kinematic data, we calculate a net normal slip of at least 9.5 km across the Hope fault (figure 2). Balancing the eroded upright limb of an overturned fold in the footwall, that developed as part of the Late Cretaceous Moyie thrust system (Harrison et al. 1986; Fillipone et al. 1992), implies that dip slip may even be as great as 12 km (figure 2).

Although these kinematic data suggest that at least the last episode of movement along the Hope fault was normal slip, earlier it might have experienced strike-slip movement. However, structures typically associated with strike-slip faulting such as Riedel and conjugate Riedel shears, en echelon folds, and minor strike-slip faults (Sylvester 1988) are not observed in the mapped area or on regional maps. Minor normal faults with displacements of a few meters to tens of meters are the only structures observed in the footwall of the Hope fault. It is unlikely that all evidence for strike slip in the Hope fault zone was completely wiped out during later normal faulting; therefore, normal-sense dip slip is the only type of movement that can be inferred from structural evidence along the Hope fault.

Estimating Dip Slip from Thermochronometry

Plutons intruded into the hanging wall and foot-wall of a normal fault that has experienced significant and rapid dip-slip displacement should have different thermal histories. In many simple cases, the resulting thermal history contrasts may be interpreted in terms of a total fault offset. Not all plutons exposed across a dip-slip fault need show abrupt changes in cooling rates, as this is a function of the timing of fault movement; an additional
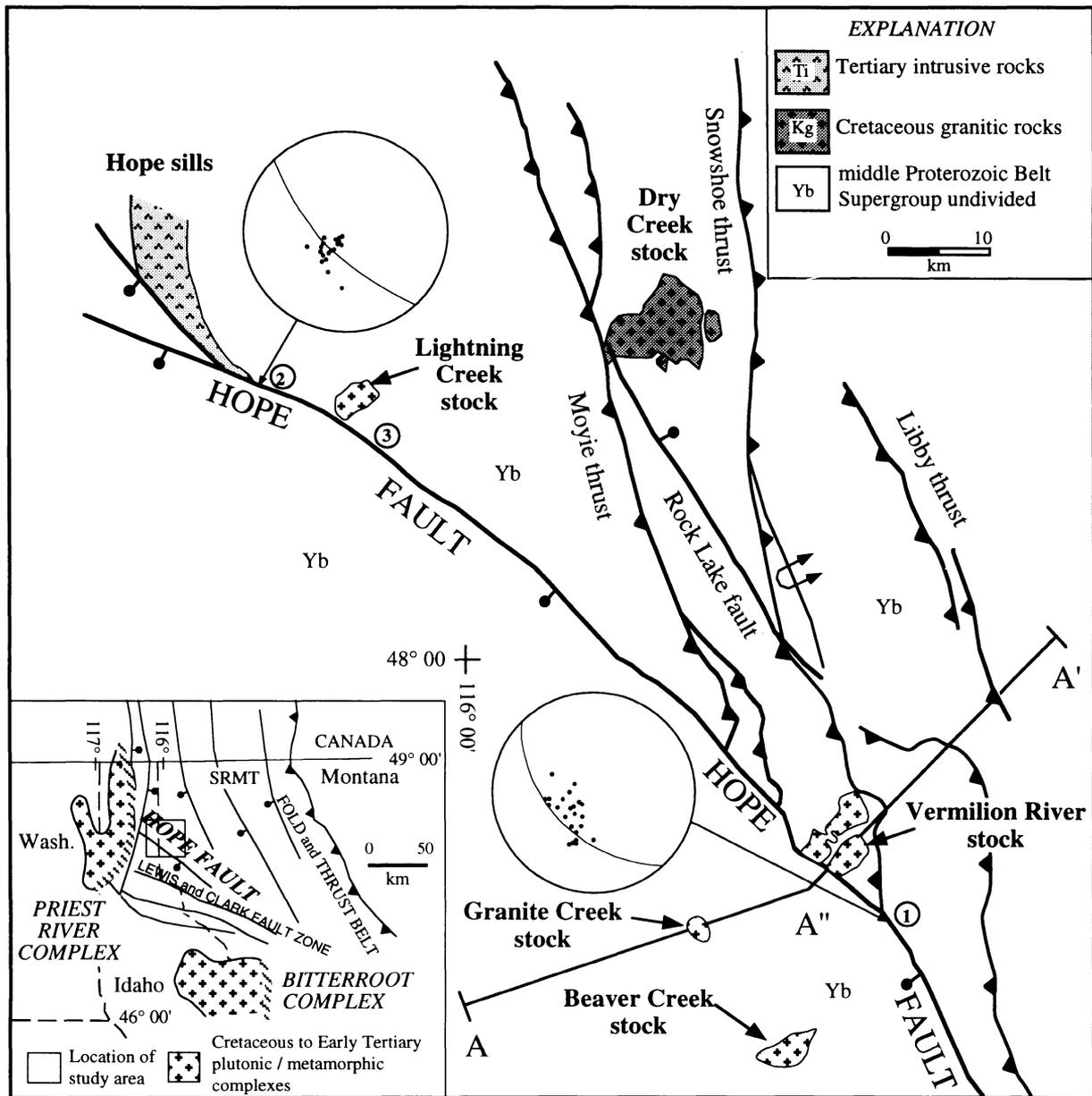
Figure 1. Regional geologic map highlighting plutons, major thrust faults, and normal faults. Striations along the Hope fault at two locations are plotted on lower hemisphere equal-area projections. Numbered locations are as follows: (1) Blueside, MT; (2) East Hope, ID; (3) Webb Creek, ID. Inset, a simplified map of the study area. Diagonal dashed pattern on the east margins of the Priest River and Bitterroot core complexes shows location of detachment fault/mylonite zone.

factor that must be considered in reconstruction of fault movement histories. Some commonly encountered faulting scenarios and their hypothetical cooling histories are shown in figure 3.

Thermal histories of orogenic belts typically involve a period of rapid heating or cooling that can be related to vertical transport of rocks to either greater or shallower crustal levels by faulting (En-

gland and Richardson 1978; England and Thompson 1984, among many others). In the past it has been very difficult to assess the thermal histories of rocks from geologic settings that lack diagnostic metamorphic mineral assemblages or thermal maturation indicators. The Belt basin with its generally low grade of metamorphism is such a case. The metamorphic facies of much of the Belt strata
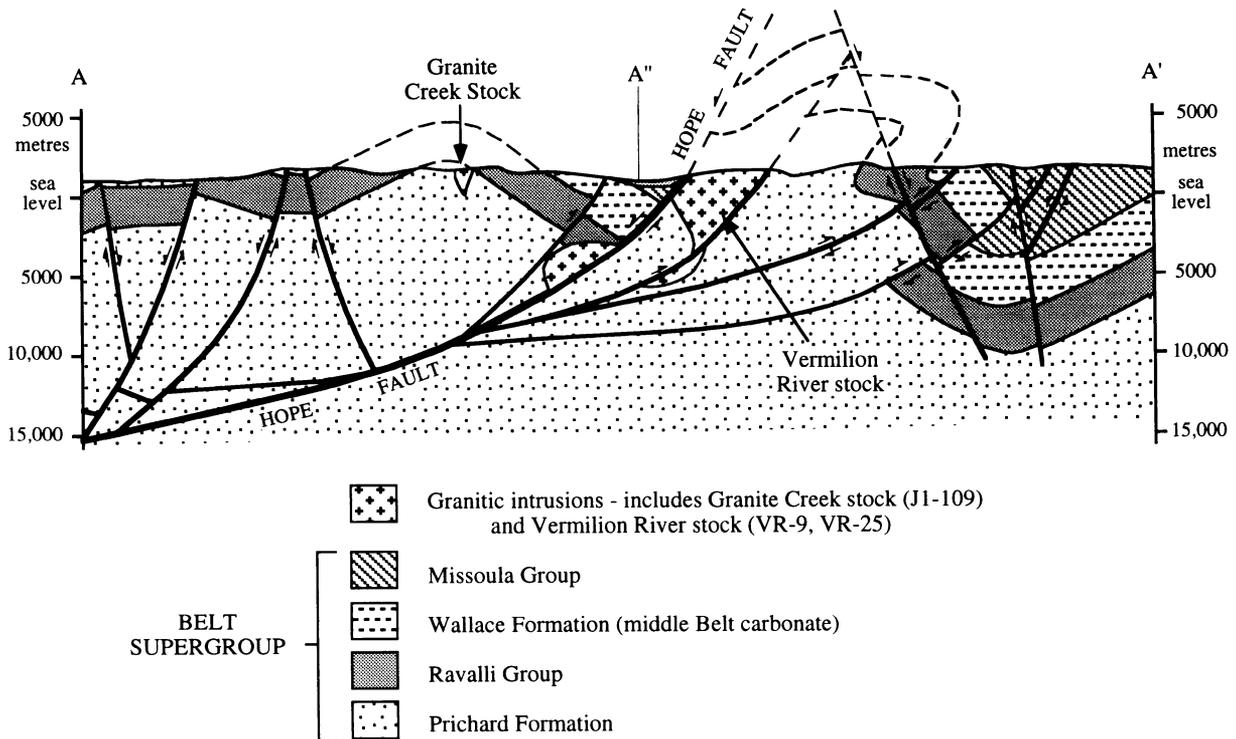
Figure 2. Cross-section A-A' constructed using offsets of stratigraphic units from Harrison et al. (1986) and unpublished mapping (Yin 1991; Fillipone et al. 1992). Plutons shown in the cross-section are those discussed in the text (not present in the cross-section is the Beaver Creek stock, figure 1). See figure 1 for cross-section location.
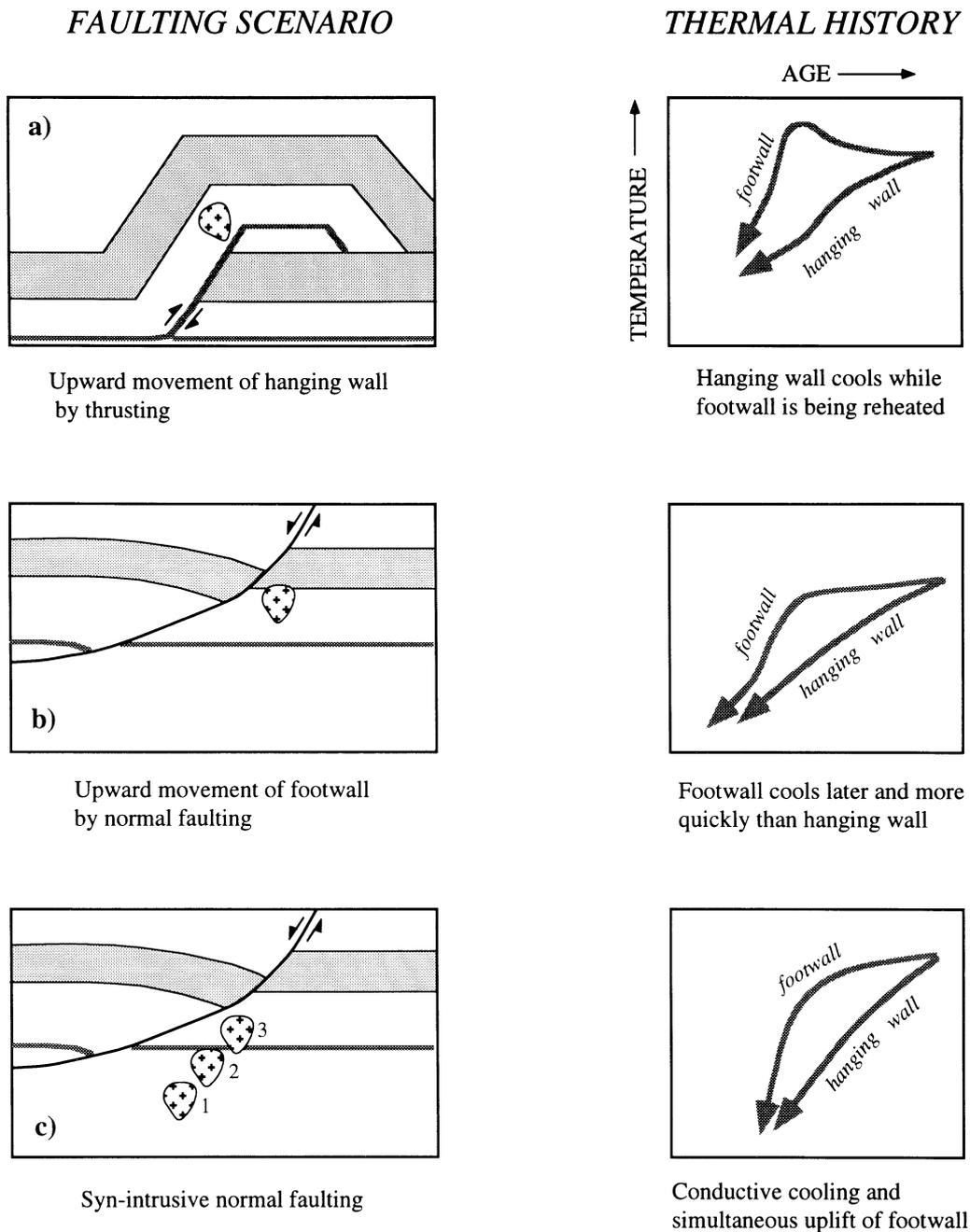
is unclear (Harrison et al., 1974). The Belt strata have frequently been cited as being "unmetamorphosed" (Rhodes and Hyndman 1984; Rehrig et al. 1987; Yoos et al. 1991). Like other rocks of their age (ca. 1300–1600 Ma, Armstrong et al. 1987), the Belt strata have insufficient organic carbon for the development of vitrinite or other kerogens that could be used to determine aspects of their thermal history (Bustin 1989). Fission track thermochronology is possible, but would provide only a lower range of closure temperatures and their associated ages (typically 100°–250°C; Ravenhurst and Donelick 1992), which is below the range of temperatures where many upper to mid-crustal rocks undergo translation and deformation. K-feldspar thermochronology, on the other hand, can potentially record closure temperatures between ~400° and 150°C, revealing subtle features of a continuous time-temperature path. In the present study area, granitic plutons containing abundant K-feldspar were emplaced at different structural levels (figures 1, 2), and then later uplifted during extensional faulting. These rocks are suitable materials for $^{40}Ar/^{39}Ar$ thermochronometry and for an investigation of the thermal history. Tables containing the argon isotopic data can be obtained

free of charge from *The Journal of Geology*, upon request.

Thermal Histories

Multi-Domain Theory. $^{40}Ar/^{39}Ar$ step-heating experiments of K-feldspar informs us on the thermal history if we assume that thermally activated volume diffusion (Arrhenius-type law) governs the laboratory outgassing of the feldspar crystals (Zeitler 1987; McDougall and Harrison 1988; Lovera et al. 1991). The multi-domain diffusion theory predicts the presence of differing length scales for diffusion of argon in feldspars (Lovera et al. 1991). Lovera (1989) suggested that the domain size (ρ) and volume fraction (ϕ) of each domain should be embodied in the step-heating data and proposed a new type of plot, the $\log r/r_o$ plot, that can reveal the distribution of the individual domains. The $\log r/r_o$ plot compares the log of the deviation of the diffusion law (Arrhenius) with that of a "reference domain" whose activation energy (E) and frequency term ($\log D_o/r^2$) are estimated from the lower temperature data (usually 400°–700°C) of the step-heating experiment.

The distribution of the individual diffusion do-

FAULTING SCENARIO

THERMAL HISTORY

AGE ⟶

a)

Upward movement of hanging wall
by thrusting

Hanging wall cools while
footwall is being reheated

b)

Upward movement of footwall
by normal faulting

Footwall cools later and more
quickly than hanging wall

c)

Syn-intrusive normal faulting

Conductive cooling and
simultaneous uplift of footwall

Figure 3. Sketches of various hypothetical dip-slip faulting scenarios and their expected time-temperature paths: (a) thrusting; (b) normal faulting; (c) syn-intrusive normal faulting. In each diagram a small pluton is shown that could potentially be used to trace the cooling history of a fault block if it became available for thermochronometry. Multiple plutons could be imagined throughout the cross-section that could give arrays of temperature-time paths after erosion (and uplift) brings them to the surface.

mains is estimated by fitting the experimental Arrhenius and log r/r_o plots using expressions derived for fractional release of ^{39}Ar (Lovera et al. 1989). From the domain distribution a cooling history can be determined by iterative calculation of an age spectrum that incorporates the domain distribution parameters (see Lovera 1992, p. 790). The

spectrum of closure temperatures (herein referred to as T_c) provided by the forward modeling of the age spectrum simulates the geologic thermal history that the K-feldspar crystals experienced in nature. Harrison et al. (1991) noted that apparent differences in activation energies were resolvable from the Arrhenius data. In our initial trials using

multiple activation energies, we noted a generally high range of closure temperatures in the cooling history models in excess of the temperatures anticipated from considerations of regional metamorphic grade. We therefore have employed the single-activation-energy approach, which results in temperatures more in accord with the lower greenschist assemblages that are widespread in the Belt.

The sensitivity of the fit of an individual age spectrum and log r/r_o plot varies from sample to sample. In our experience, minor variations in assumed cooling rates or times when rates change for a given cooling history cause drastic deviations in the model fit. The distribution parameters of the diffusion domains are determined by a numerical scheme that can be slightly altered with negligible effects on the modeled cooling history. By varying the parameters of the cooling history we can bracket a range of acceptable fits, thereby demonstrating the sensitivity of calculated age spectra to our model cooling histories.

Thermochronology Results. Granitoid plutons predating fault movement are exposed in the footwall and hanging wall of the Hope fault (figures 1, 3). Aluminum-in-hornblende geobarometry (method of Johnson and Rutherford 1989; see table 1 for results), indicates crystallization at mesozonal depths of ~10–15 km ($\Sigma 3.5$–5 kb). The youngest known intrusions cut by the fault (Hope sills, figure 1) gave a U-Pb zircon date of 58.1 ± 5.1 Ma (concordia intercept age, 95% confidence interval), and a $^{40}Ar/^{39}Ar$ hornblende date of 49 ± 1 Ma (figure 4). K-feldspars were used to derive a continuous segment of each pluton's cooling history by applying multi-diffusion domain theory (Lovera et al. 1989; Lovera et al. 1991; Harrison et

al. 1992). Combining thermochronometric results for hornblende, biotite, and K-feldspar for plutons in the foot and hanging walls, large portions of their thermal histories were retrieved. Contrasts in closure temperatures ("T_c"; see Dodson 1973) for two to three different minerals in each sample (hornblende, biotite, K-feldspar) permit construction of extended cooling histories. Volume averaged T_c's of 500° and 325°C, were used for hornblende and biotite (McDougall and Harrison 1988). Dates were obtained using techniques described in Baldwin and Harrison (1992) and Harrison et al. (1992).

Two plutons each from the footwall and hanging wall of the Hope fault were investigated by $^{40}Ar/^{39}Ar$ thermochronometry to test the hypothesis of major dip slip. Dating of hornblende and biotite from the hanging wall plutons gave apparent ages of ~93 Ma (Beaver Creek stock) and 110 ± 2 Ma (Granite Creek stock), respectively (figure 5a,b). In the footwall, the composite Vermilion River stock (herein interpreted as two separate plutons) gave one hornblende apparent age of 114 ± 2 Ma (plateau age; 75.2% of total gas; figure 5c, sample VR-9) from the largest pluton, with a second age spectrum for a smaller pluton indicating a minimum age of ~140 Ma (figure 5d, sample VR-25). The stock therefore appears to be at least as old as 114 Ma and may have much older components, assuming the latter date is reliable.

Step-heating results for the hanging wall K-feldspars are presented in figures 6 and 7. K-feldspar age spectra for the two plutons (figures 6a, 7a) have strongly contrasting thermal histories (Figures 6d, 7d). An Arrhenius plot of ^{39}Ar diffusivities versus reciprocal absolute temperature (calculated assuming a plane slab geometry for the diffusion domains) yielded frequency terms (log D_o/r^2) and activation energies (E) for the initial low temperature steps of 6.3 s^{-1} and 46.6 kcal/mol, and 6.5 s^{-1} and 47.9 kcal/mol, for the Beaver Creek (sample BC-1, figure 6a) and Granite Creek (sample J1-109, figure 7a) stocks, respectively. Seven domains were chosen to obtain the fit to the log (r/r_o) plot for sample BC-1, and eight domains for sample J1-109; their activation energies are given in figures 6c and 7c. Thermal modeling indicates cooling of the Beaver Creek and Granite Creek stocks to temperatures of ~270° by about 80 Ma (figures 6d, 7d).

K-feldspars from the footwall pluton yield age spectra typical of slow cooling between about 30% to 90% (VR-9), and 20 to 80% ^{39}Ar released (VR-25), at rates <1°C/Ma, to nearly isothermal (figures 8d, 9d). The flat portion of the spectrum be-

Table 1. Crystallization Pressures from Plutons Adjacent to the Hope Fault, Northwest Montana, Determined by Al-in-Hornblende Geobarometry

| Sample	Rim (R) or Core (C)	Footwall (FW) or Hanging Wall (HW)	Pressure (kb)
Granite Creek stock (J1-109)	R	HW	4.2 to 5.4
Vermilion River stock (VR-9)	R	FW	3.4 to 4.1
Vermilion River stock (VR-25)	R	FW	3.3 to 4.8
Lightning Creek stock (LC-34)	R	FW	4.6 to 5.5

Note. Pressures of crystallization estimated from the aluminum-in-hornblende geobarometer of Johnson and Rutherford for hanging wall and footwall plutons along the Hope fault in figure 1a. Errors in the calibration are on the order of ±0.5 kb.
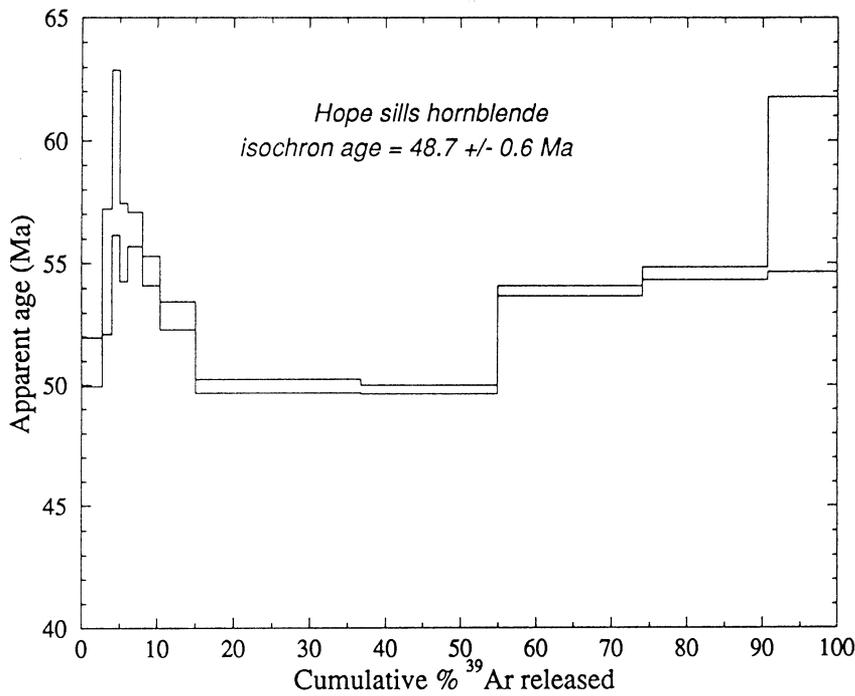
Figure 4. $^{40}Ar/^{39}Ar$ age spectrum of hornblende from the Hope sills (sample SPG-6), collected from the footwall of the Hope fault just west of Hope, Idaho on Highway 200. An inverse isochron age of 48.7 ± 0.6 Ma (MSWD = 28.9; $^{40}Ar/^{36}Ar_{trapped}$ = 328 ± 8). The two youngest steps (49–50 Ma) correspond to the highest radiogenic component in the step-heating data (83% $^{40}Ar^{*}$, 39.9% gas released).
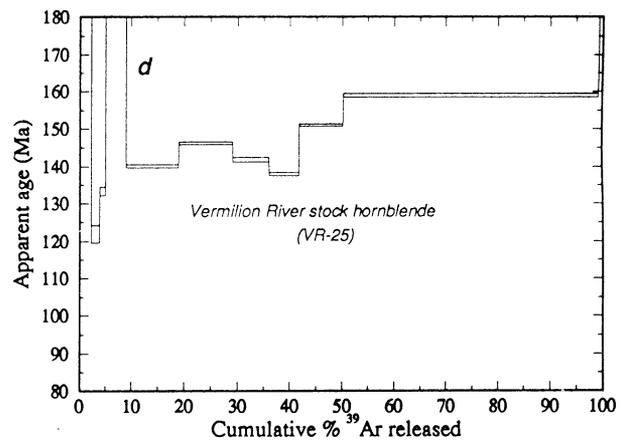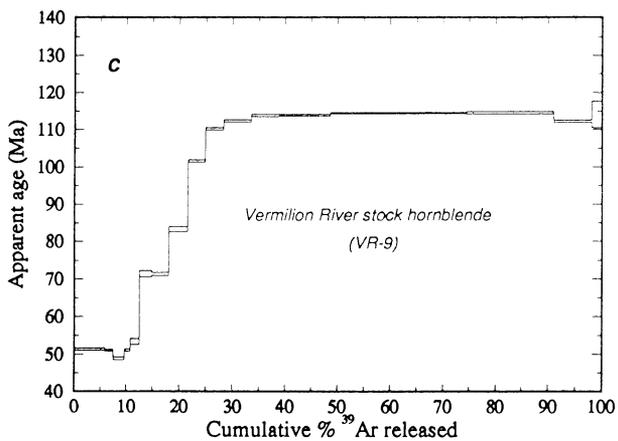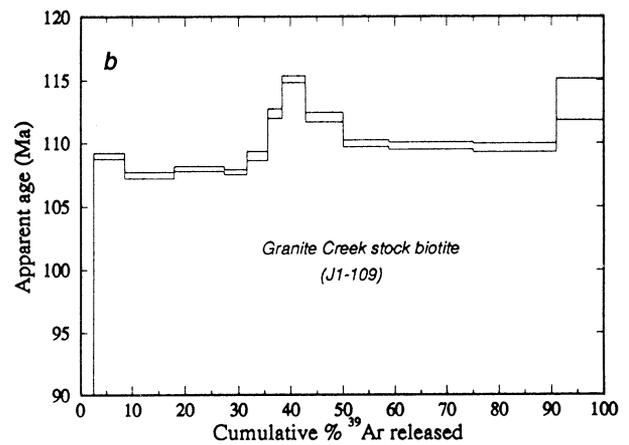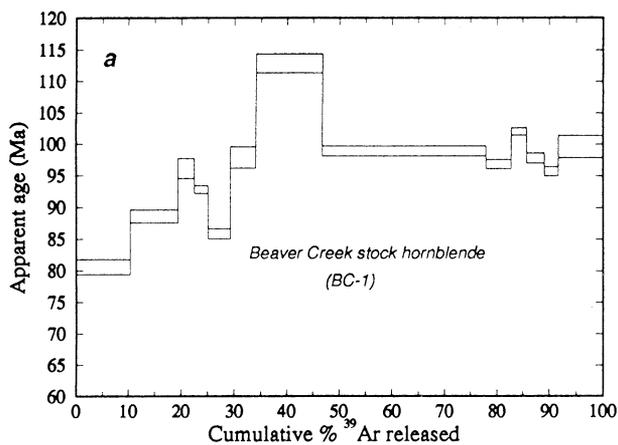
Figure 5. $^{40}Ar/^{39}Ar$ age spectra of hornblende and biotite from the plutons discussed in the text and shown in figure 1. (*a*) Beaver Creek stock hornblende (BC-1); (*b*) Granite Creek stock biotite (J1-109); (*c*) Vermilion River stock hornblende (VR-9); and VR-25 shown in (*d*).
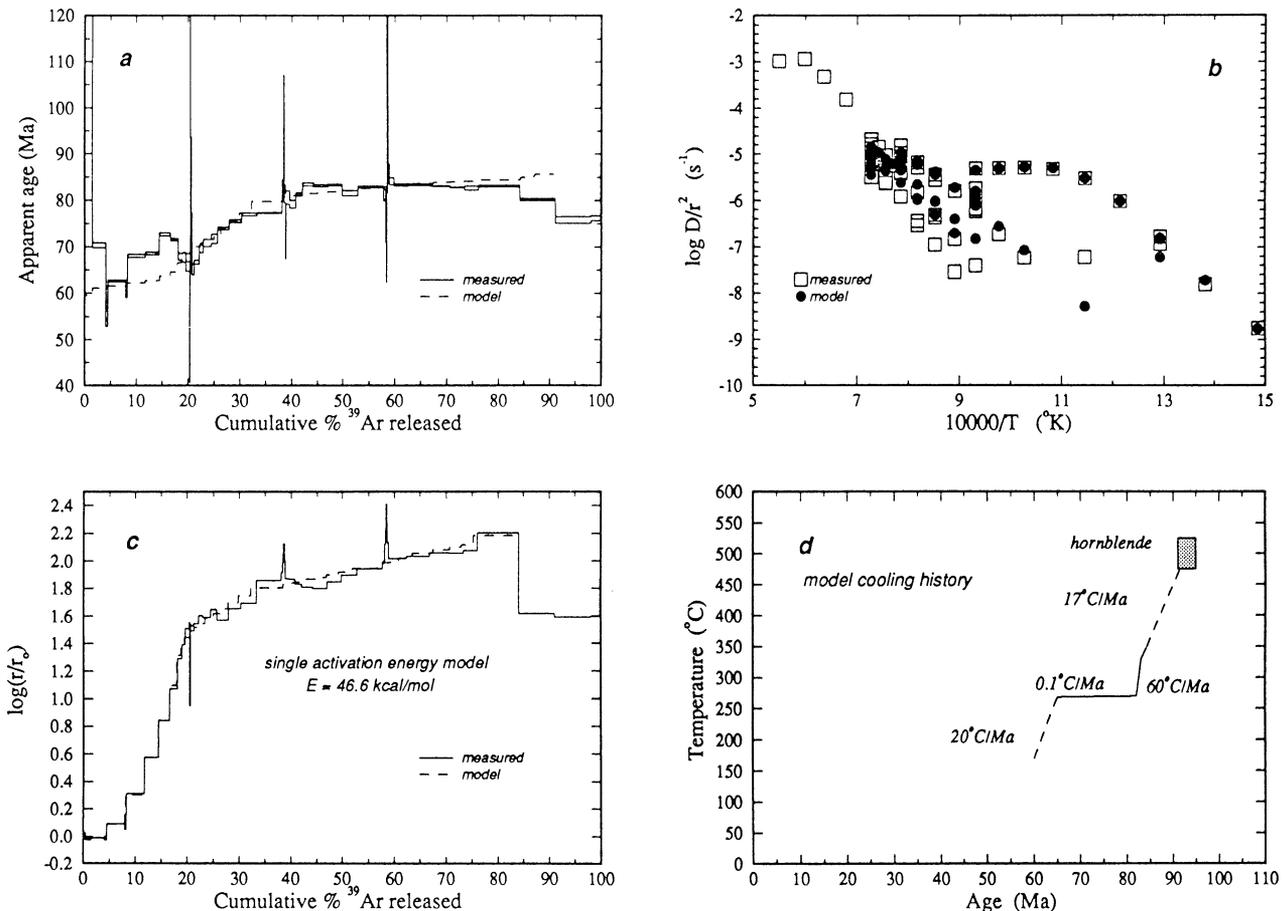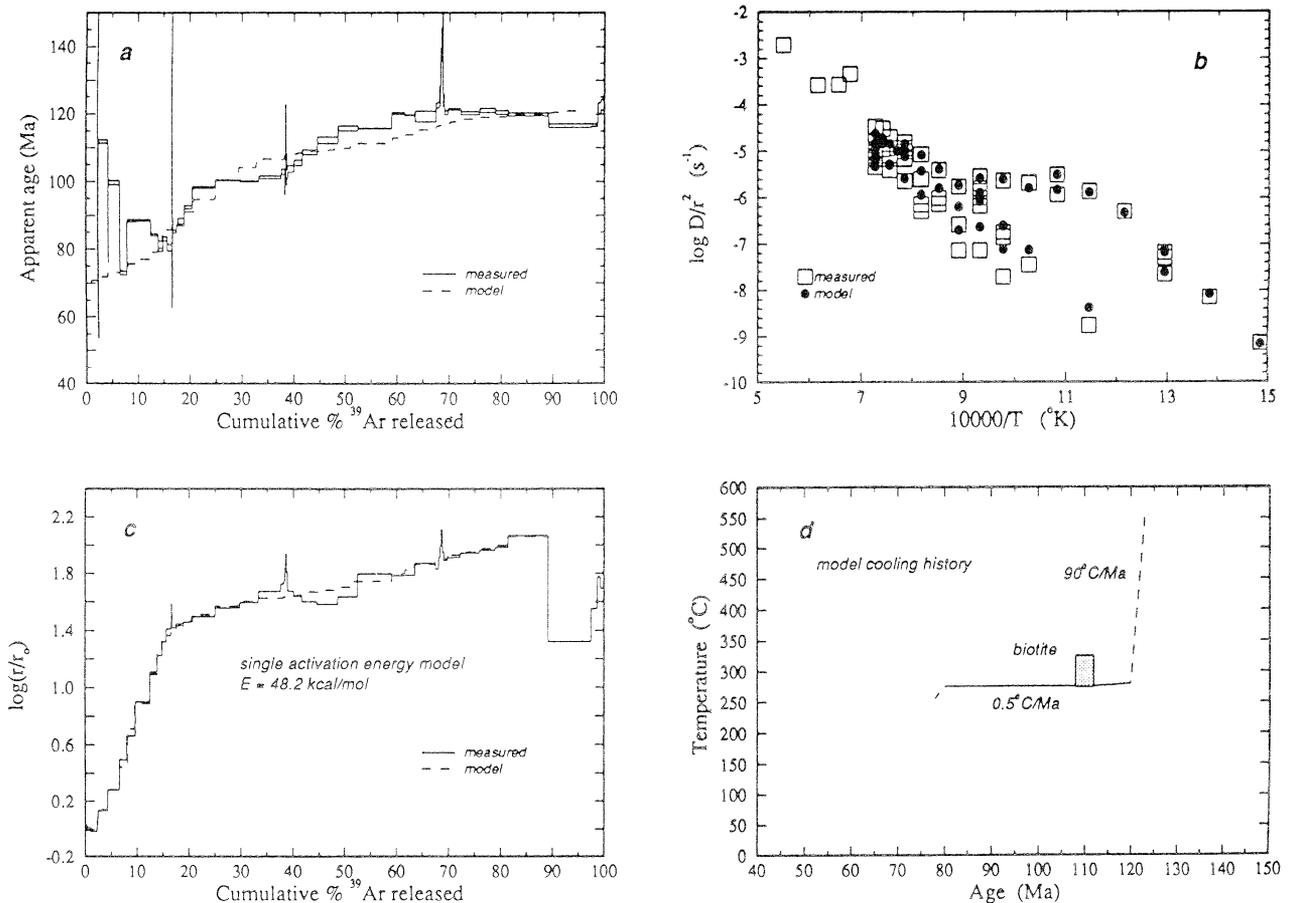
Figure 6. (a) $^{40}Ar/^{39}Ar$ K-feldspar age spectrum of the hanging wall Beaver Creek pluton; (b) Arrhenius plot; (c) log (r/r_o) plot; and (d) cooling history with the hornblende apparent age and closure temperature range. Solid lines in (a) and (c) indicate actual data, dashed lines are model fits. In (b) the last four data points are not used in the model Arrhenius plots as the sample had begun to melt. Solid lines in (d) show cooling history model results, with dotted segments where no data are available from the K-feldspar.

tween 7% and 30% gas release (sample VR-9, figure 8a) is indicative of rapid cooling at rates of ~60°C/Ma, beginning at 40 Ma (figure 8d). Initial release of excess argon (0 to 7%) precludes use of this part of the spectrum for analysis of the thermal history. K-feldspar of sample VR-25 yields a nearly identical cooling history corroborating this result and extending evidence for rapid cooling at rates of ~60°C/Ma down to 36 Ma (figure 9d).

Sensitivity tests were carried out to determine the effects of small changes in the cooling history on model fits to the K-feldspar age spectra. Because there rarely is a perfect fit of the model age spectrum with the age spectrum calculated from the step-heating data, we have attempted to show how sensitive the models are to assumed cooling history details. In figure 8a (VR-9 K-feldspar), model 1 is a synthetic age spectrum generated using a thermal history with a cooling rate of 22°C/Ma,

between 71–70 Ma. Varying the rate by ±2°C/Ma results in substantial deviations, making the model age spectrum either younger (20°C/Ma, figure 8a, model 2) or older (figure 8a, model 3). These variations show that the envelope of possibilities for this particular thermal history model is in the range of ±5°C/Ma for a substantial amount of the gas released. The minor mismatches of the model with the measured age spectrum were similarly evaluated for the second K-feldspar sample from the Vermilion River stock (figure 9). The cooling rate of 16°C/Ma beginning at 71 Ma in model 1 is increased by 1°C to 17°C/Ma in model 2 (figure 9d). The resulting shift in the model age spectrum is dramatic (figure 9a), yet the thermal history is essentially indistinguishable from model 1. Of greatest importance is the fact that the overall form of the thermal history with an older stage of fast cooling followed by very slow cooling and
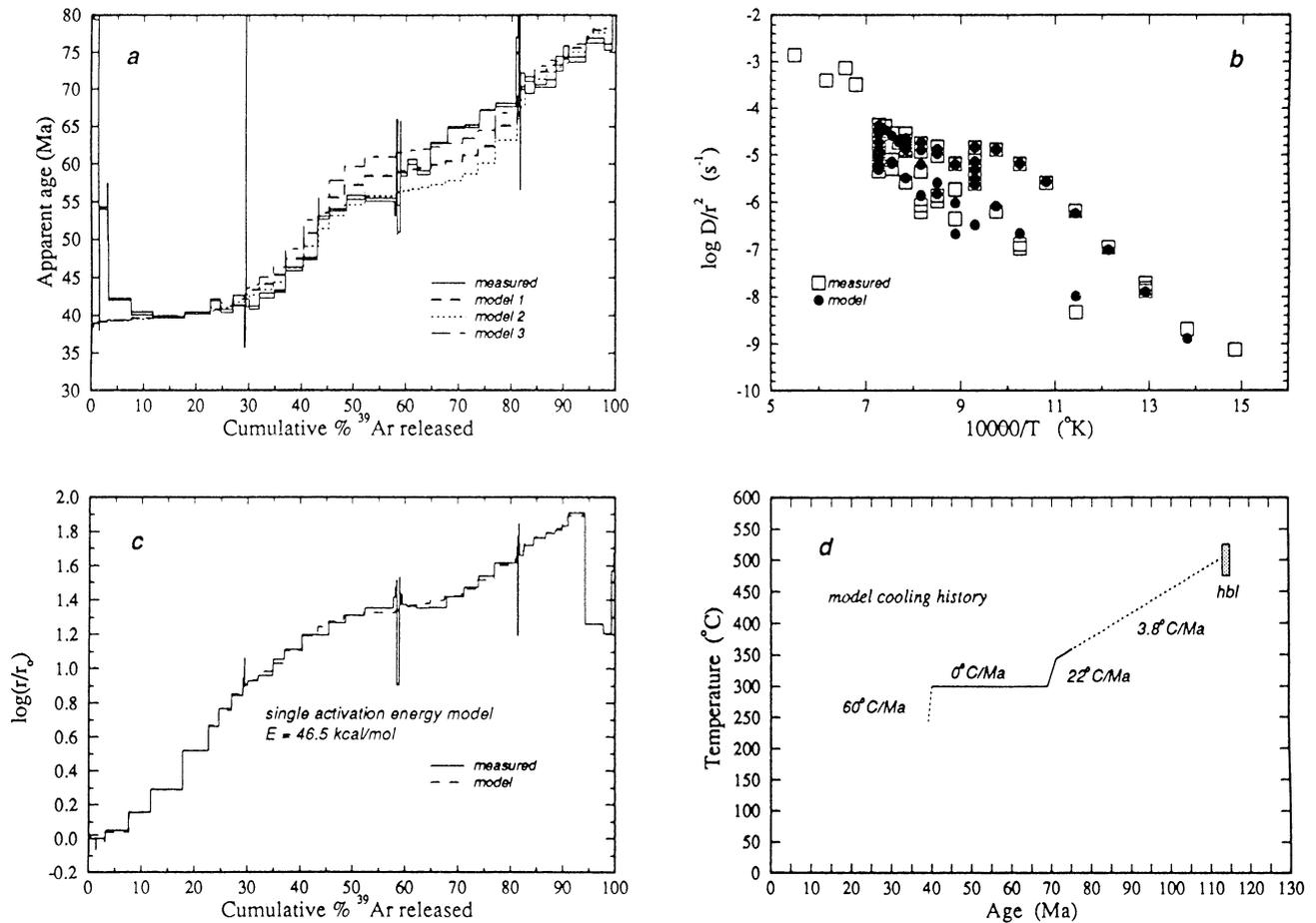
Figure 7. (a) K-feldspar age spectrum of the hanging wall Granite Creek pluton; (b) Arrhenius plot; (c) log (r/r_o) plot; and (d) cooling history with the biotite apparent age and closure temperature range. The model age spectrum in (a) requires slow cooling throughout and is difficult to fit without artificially introducing a large number of very subtle complexities that do not significantly alter the general cooling history presented.

then another interval of fast cooling must be present in order to generate even a loose fit to the age spectrum.

Discussion

The pre-kinematic nature and slow cooling histories of both the footwall and hanging wall plutons during the Cretaceous, followed by rapid cooling of the footwall plutons in late Eocene suggests that a component of normal slip on the Hope fault was the likely cause of the rapid cooling. A summary of all the K-feldspar model cooling histories is presented in figure 10. K-feldspar closure temperatures for the flat segments of footwall plutons cooling histories before the 40 and 36 Ma segments (figure 10) are ~300°C, indicating that these rocks probably were at depths of 9–14 km at that time, whereas the hanging wall rocks last experienced that temperature at about 65 to 80 Ma or earlier. From the thermal modeling presented, we inter-

pret that the footwall and hanging wall cooling histories (and age spectra) attain their greatest contrasts in the interval from about 68 to 80 Ma. In that interval, calculated closure temperatures of the footwall and hanging wall samples differ by a minimum of 60°C and a maximum of 140°C (figure 10). A temperature contrast of the order of 100°C corresponds to a pre-40 Ma depth difference of 3 to 5 km, assuming average thermal gradients of 25 ± 5°C/km. The model thermal history of the footwall pluton indicates rapid cooling at 40 Ma, with movement being initiated after ~49 Ma (^{40}Ar/^{39}Ar hornblende age of the Hope sills). Combining the inferred vertical component of displacement from the differential cooling histories with the average observed dip angle of the Hope fault (30°–50°) suggests a dip-slip component of about 4 to 10 km, which is compatible with observed offsets of Belt strata (figure 2). Field relationships, the hornblende age of the cross-cut Hope sills, and modeled ^{40}Ar/^{39}Ar cooling histories are consistent with an inter-
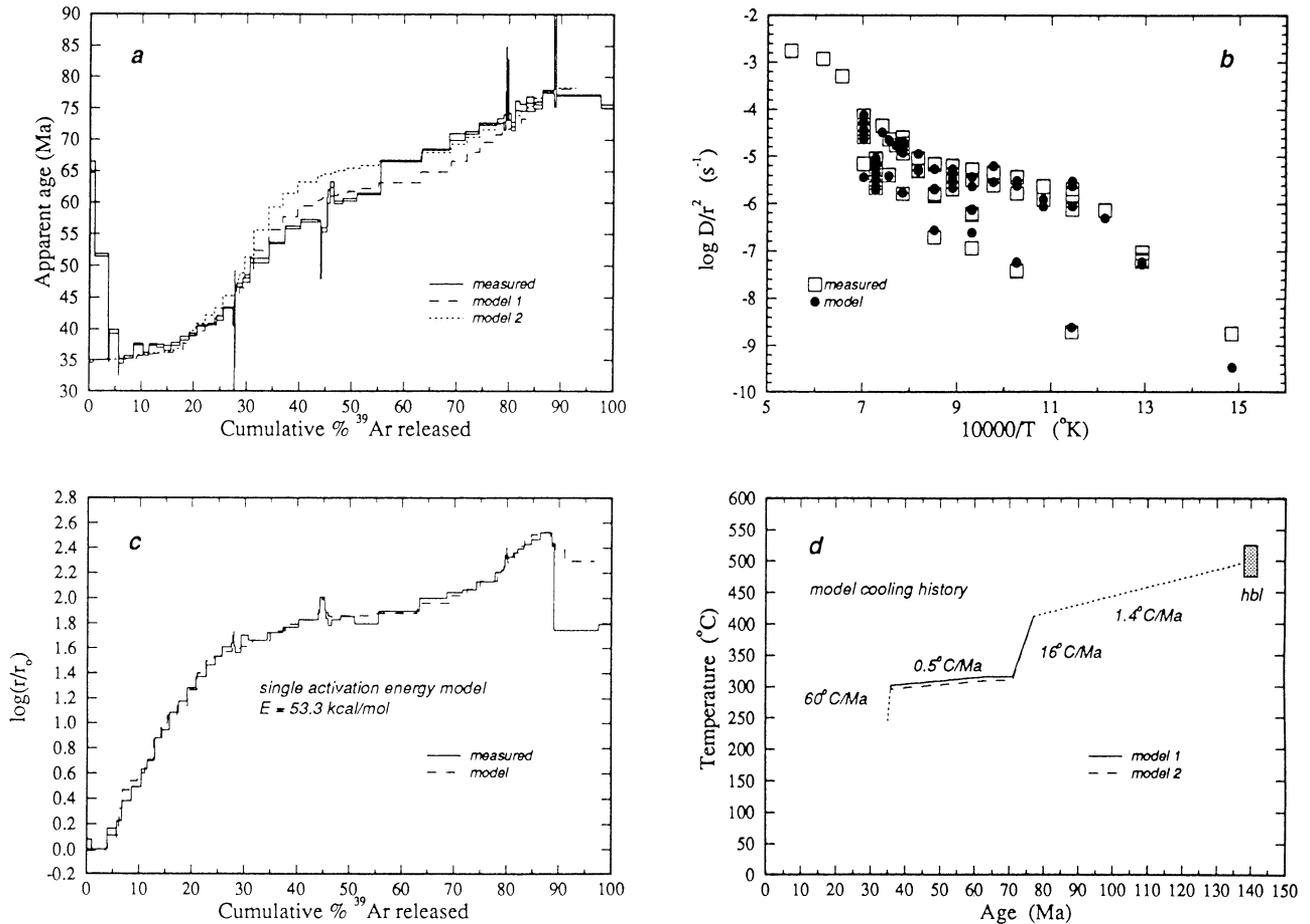
Figure 8. (a) K-feldspar age spectrum of the footwall Vermilion River stock, sample VR-9; (b) Arrhenius plot; (c) log (r/r) plot; and (d) cooling history with the hornblende apparent age and closure temperature range. The age spectra of models 1–3 are sensitivity tests discussed in the text.

pretation of rapid uplift of the footwall in the Late Eocene.

These findings impact the diverse previous regional interpretations of cooling histories and their causes as well as tectonic models for Tertiary extension in the northern U.S. Cordillera. To some authors the fault originally was a Precambrian structure that experienced reactivation during the Mesozoic and Tertiary (Harrison et al. 1972, 1974, 1986, 1992; Wallace et al. 1990). Its western part lies north of the Lewis and Clark line (figure 1), a system of reverse, normal and strike-slip faults (Wallace et al. 1990). No consensus exists whether or not it is part of the Lewis and Clark line (Calkins 1909; Billingsley and Locke 1965; Reynolds 1979). Because of its age and apparent significant normal dip slip, the fault strongly resembles normal faults of the southern Rocky Mountain trench fault system, and thus may not be a part of the Lewis and Clark line proper. Many recent interpretations of the Lewis and Clark line envisage an episode of right slip to accommodate Tertiary extension re-

lated to core complexes development to the north and south of the line (Rehrig et al. 1987; Hyndman et al. 1988; Doughty and Sheriff 1992; Hodges and Applegate 1993). Because the available kinematic data suggest that the latest movement on these faults was mostly reverse or normal slip (Yin and Fillipone 1994), it appears that significant Tertiary strike-slip on the western Lewis and Clark line cannot serve to link domains of regional extension. Interpretation of kinematic data and thermochronometry from our study suggests that during the early to mid-Tertiary, the Hope was a normal dip-slip fault, thus also precluding Tertiary right-slip.

The present data also challenge the concept of Tertiary "resetting" of older Mesozoic (?) ages in northwest Montana. Miller and Engels (1975) and Armstrong et al. (1987) defined a region of Tertiary resetting of older K/Ar ages that extends to the eastern margin of the Priest River complex in northern Idaho. Our data are from outside the zone where purported outgassing by a thermal pulse in the Tertiary took place (see Armstrong et al. 1987).

Figure 9. (a) K-feldspar age spectrum of the footwall Vermilion River stock, sample VR-25; (b) Arrhenius plot; (c) log (r/r$_o$) plot; and (d) cooling history with the hornblende apparent age and closure temperature range. The age spectra of models 1 and 2 are sensitivity tests discussed in the text.
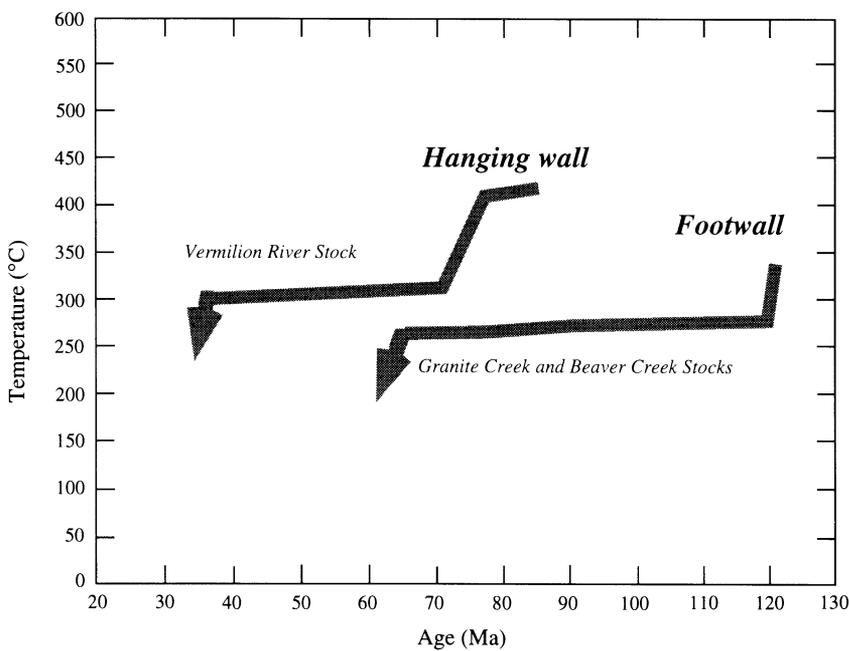
Figure 10. Summary time-temperature diagram showing the differential K-feldspar model thermal histories from the footwall and hanging wall plutons. The differential cooling histories result in a minimum temperature contrast of 80°C and a maximum contrast of 140°C. Interpretation of this contrast in terms of the vertical component of displacement indicates that between 4–10 km of dip slip occurred on the Hope fault in the Late Eocene.

We nevertheless find that late Eocene rapid cooling ages are preserved outside the zone of resetting proposed by Armstrong et al. (1987). The simplest interpretation consistent with the geologic data is that the footwall cooled slowly throughout the latest Cretaceous, then rapidly cooled in response to denudation and/or erosion. We suggest that extent of this "resetting" event be re-evaluated in light of the rapid cooling we have detected in samples east of the Priest River complex.

Conclusions

Recent advances in our ability to derive thermal history information from K-feldspar $^{40}Ar/^{39}Ar$ results (Lovera et al. 1991; Harrison et al. 1992; Leloup et al. 1993) create new possibilities for applying the method described in this paper to tectonic problems involving dip-slip faulting. Small plutons that behave as "thermal monitors," provide a means of tracking the cooling history of rocks in diverse geological settings and estimating vertical displacements caused by normal faulting. The plutons we have studied from the footwall of the Hope fault (Fillipone 1993), regardless of their crystallization ages, show rapid cooling between 45–40 Ma, consistent with a tectonic explanation for footwall cooling. Similar ages of extensional faulting at other localities in the northwest U.S. (e.g., S. Rocky Mountain trench, Constenius 1981; Priest River complex, Armstrong et al. 1987; Bitterroot complex, Chase et al. 1983) suggest a common tectonic evolution and perhaps kinematic linkage existed among these mid-Tertiary extensional terranes. The lack of evidence for strike slip along the Hope fault, and in the western Lewis and Clark line in general, invites a reassessment of how this common episode of extension was accomplished.

REFERENCES CITED

Armstrong, R. L.; Parrish, R. R.; van der Heyden, P.; Reynolds, S. J.; and Rehrig, W. A., 1987, Rb-Sr and U-Pb geochronometry of the Priest River metamorphic complex—Precambrian X basement and its Mesozoic-Cenozoic plutonic-metamorphic overprint, northeastern Washington and northern Idaho: Washington Div. Geol. Earth Res. Bull., v. 77, p. 15–40.

Baldwin, S. E., and Harrison, T. M., 1992, The P-T-t history of blocks in serpentinite-matrix melange, west-central Baja California: Geol. Soc. America Bull., v. 104, p. 18–31.

Billingsley, P., and Locke, A., 1939, Structure of Ore Districts in the Continental Framework: New York, American Inst. Mining Metal. Eng., 51 p.

Bustin, R. M., 1989, Diagenesis of kerogen, in Hutcheon, I., ed., Short course in burial diagenesis: Mineral. Assoc. Canada, Short Course Handbook, v. 15, p. 1–38.

Calkins, F. C., 1909, A geological reconnaissance in northern Idaho and northwestern Montana, U.S. Geol. Survey Bull., 384, 112 p.

Chase, R. L.; Bickford, M. E.; and Arruda, E. C., 1983, Tectonic implications of Tertiary intrusion and shearing within the Bitterroot dome, northeastern Idaho batholith: Jour. Geology, v. 91, p. 462–470.

Constenius, K., 1982, Relationship between the Kishenehn Basin, and the Flathead listric normal fault system, and the Lewis thrust salient: Rocky Mountain Assoc. Geol., p. 817–830.

Coney, P. J., 1980, Cordilleran metamorphic core complexes: an overview: Geol. Soc. America Mem. 153, p. 7–31.

Dodson, M. H., 1973, Closure temperature in cooling geochronological and petrological systems: Contrib. Mineral. Petrol., v. 40, p. 259–274.

Doughty, P. T., and Sheriff, S. D., 1992, Paleomagnetic evidence for an echelon crustal extension and crustal rotations in western Montana and Idaho: Tectonics, v. 11, p. 663–671.

England, P. C., and Richardson, S. W., 1977, The influence of erosion upon the mineral facies of rocks from different metamorphic environments: Jour. Geol. Soc. London, v. 134, p. 201–213.

—— and Thompson, A. B., 1984, Pressure-temperature-time paths of regional metamorphism I. Heat transfer during the evolution of regions of thickened continental crust: Jour. Petrol., v. 25, p. 894–928.

Fillipone, J. A., 1993, Tectonic and thermochronologic evolution of the Cabinet and Selkirk Mountains, northwest Montana and northeast Idaho: Unpub. Ph.D. dissertation, University of California, Los Angeles, 341 p.

——; Harrison, T. M.; Sample, J. C.; and Yin, A., 1992, Thermochronological evolution of the Hope and Moyie fault systems, northwest Montana and northeast Idaho: Geol. Soc. America Abs. with Prog., v. 24, no. 6, p. 11.

Harms, T. A., and Price, R. A., 1992, The Newport fault,

Eocene listric normal faulting, mylonitization, and crustal extension in northeast Washington and northwest Idaho: Geol. Soc. America Bull., v. 104, p. 745–761.

Harrison, J. E.; Griggs, A. B.; and Wells, J. D., 1974, Tectonic features of the Precambrian Belt Basin and their influence on post-Belt structures: U.S. Geol. Survey Prof. Paper 866, 15 p.

———; ———; and ———, 1986, Geology and Structure Map of the Wallace 1° × 2° Quadrangle, Montana and Idaho: U.S. Geol. Survey Misc. Invest. Series I-1509.

———, and Jobin, D. A., 1963, Geology of the Clark Fork quadrangle, Idaho-Montana: U.S. Geol. Survey Bull., v. 1141–1427.

———; Kleinnkopf, M. D.; and Obradovich, J. D., 1972, Tectonic events at the intersection between the Hope fault and the Purcell trench, northern Idaho: U.S. Geol. Survey Prof. Paper 719, 24 p.

Harrison, T. M.; Chen W.; Leloup, P. H.; Ryerson, F. J.; and Tapponier, P., 1992, Early Miocene transition in deformation regime within the Red River fault zone, Yunnan, and its significance for Indo-Asian tectonics: Jour. Geophys. Res., v. 97, p. 7159–7182.

Harrison, T. M.; Lovera, O. M.; and Heizler, M. T., 1991, ^{40}Ar/^{39}Ar results for alkali feldspars containing diffusion domains with differing activation energy: Geochim. Cosmochim. Acta, v. 55, p. 1435–1448.

Hodges, K. V., and Applegate, J. D., 1993, Age of Tertiary extension in the Bitterroot metamorphic core complex, Montana and Idaho: Geology, v. 21, p. 161–164.

Hyndman, D. W.; Alt, D.; and Sears, J. W., 1988, Post-Archean metamorphic and tectonic evolution of western Montana and northern Idaho: in Ernst, W. G., ed., Metamorphic and tectonic evolution of the western Cordillera, Conterminous United States (Ruby Volume 7): Englewood Cliffs, N.J., Prentice-Hall, p. 332–361.

Johnson, M. C., and Rutherford, M. J., 1989, Experimental calibration of the Aluminum-in-hornblende geobarometer with application to Long Valley caldera (California) volcanic rocks: Geology, v. 17, p. 837–841.

Leloup, P. H.; Harrison, T. M.; Ryerson, F. J.; Chen, W.; Li, Qi; Tapponier, P.; and Lacassin, R., 1993, Structural petrological and thermal evolution of a Tertiary ductile strike-slip shear zone, Diancang Shan, Yunnan: Jour. Geophys. Res., v. 98, p. 6715–6743.

Lovera, O. M., 1992, Computer programs to model ^{40}Ar/^{39}Ar diffusion data from multidomain samples: Computers and Geosci., v. 18, p. 789–813.

———; Richter, F. M.; and Harrison, T. M., 1989, The ^{40}Ar/^{39}Ar thermochronometry for slowly cooled samples having a distribution of domain sizes: Jour. Geophysical Res., v. 94, p. 17,917–17,935.

———; ———; and ———, 1991, Diffusion domains determined by ^{39}Ar released during step heating: Jour. Geophys. Res., v. 96, p. 2057–2069.

Lyons, J., and Snellenburg, J., 1971, Dating faults: Geol. Soc. America Bull., v. 82, p. 1749–1751.

McDougall, I., and Harrison, T. M., 1988, Geochronology and Thermochronology by the ^{40}Ar/^{39}Ar Method (Oxford Mon. Geology Geophys. 9): New York, Oxford Univ. Press, 212 p.

Miller, F. K., and Engels, J. C., 1975, Distribution and trends of discordant ages of the plutonic rocks of northeastern Washington and northern Idaho: Geol. Soc. America Bull., v. 86, p. 517–528.

Pardee, J. T., 1950, Late Cenozoic block faulting in western Montana: Geol. Soc. America Bull., v. 61, p. 359–406.

Ravenhurst, C. E., and Donelick, R. A., 1992, Fission track thermochronology: in Zentilli, M., and Reynolds, P. H., eds. Short course on low temperature thermochronology: Mineral. Assoc. Canada Short Course handbook, v. 20, p. 21–42.

Rehrig, W. A.; Reynolds, S. J., and Armstrong, R. L., 1987, A tectonic and geochronologic overview of the Priest River crystalline complex, northeastern Washington and northern Idaho: Washington Div. Geol. Earth Res. Bull. 77, p. 1–14.

Reynolds, M. W., 1979, Character and extent of Basin-Range faulting, western Montana and east-central Idaho: Rocky Mountain Assoc. Geol.–Utah Geol. Assoc. 1979 Basin and Range Symposium Guidebook, p. 185–193.

Rhodes, B. P., and Hyndman, D. W., 1988, Regional metamorphism, structure, and tectonics of northeastern Washington and northern Idaho: in Ernst, W. G., ed., Metamorphic and Crustal Evolution of the Western United States (Rubey Volume 7): Englewood Cliffs, N.J., Prentice-Hall, p. 272–295.

Smith, J. G., 1965, Fundamental transcurrent faulting in the northern Rocky Mountains: Am. Assoc. Petrol. Geol. Bull., v. 49, p. 1398–1409.

Sylvester, A. G., 1988, Strike-slip fault systems: Geol. Soc. America Bull., v. 100, p. 1666–1703.

Wallace, J. D.; Lidke, D. J.; and Schmidt, R. G., 1990, Faults of the central part of the Lewis and Clark line and fragmentation of the Late Cretaceous foreland basin in west-central Montana; Geol. Soc. America Bull., v. 102, p. 1021–1037.

Wiltschko, D. V., and Dorr, J. A., Jr., 1983, Timing of deformation in Overthrust Belt and Foreland of Idaho, Wyoming, and Utah: Am. Assoc. Petrol. Geol. Bull., v. 67, p. 1304–1322.

Yin, A., 1991, Kinematics of the Hope-Ninemile fault and its tectonic implications, northern Idaho and northwestern Montana: Geol. Soc. America Abs. with Prog., v. 23, p. 111.

———, and Fillipone, J. A., 1994, Fault kinematics of the western Lewis and Clark Line: in Belt Symposium III, Abstract Vol., Montana Bur. Geol. and Mines, p. 32.

Yoos, T. R.; Potter, C. J.; Thigpen, J. L.; and Brown, L., 1991, The Cordilleran foreland thrust belt in northwestern Montana and northern Idaho from COCORP and industry seismic reflection data: Am. Assoc. Petrol. Geol. Bull., v. 75, p. 1089–1106.

Zeitler, P. K., 1987, Argon diffusion in partially outgassed alkali feldspars: insights from ^{40}Ar/^{39}Ar analysis: Chem. Geology, v. 65, p. 167–181.